

Syntheses, Characterizations, and Properties of Electronically Perturbed 1,1'-Dimethyl-2,2'-bipyridinium Tetrafluoroborates

Dong Zhang, Eric J. Dufek, and Edward L. Clennan*

Department of Chemistry, University of Wyoming, 1000 East University Avenue, Laramie, Wyoming 82071

clennane@uwyo.edu

Received October 11, 2005



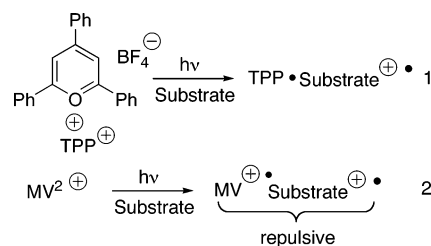
The syntheses of three new 2,2'-bipyridinium tetrafluoroborate sensitizers are reported. Their preliminary electrochemical and photophysical properties are compared to the properties of the more widely used pyrylium cation sensitizers. In addition, the first examples of triplet-triplet absorption spectra of 2,2'-bipyridinium ions are presented.

Introduction

Photoinduced electron transfer (PET) is a convenient and well-established methodology.¹ Back electron transfer (BET) in the ion pair intermediates, however, provides a significant limitation in terms of achieving energy efficiency. This problem has been addressed by using pyrylium salts such as TPP[⊕] to produce substrate radical cations that do not suffer detrimental Coulombic attraction to the reduced sensitizer² (eq 1; Scheme 1).

We recently became interested in determining if BET could be further suppressed by using dicationic sensitizers such as viologens³ and their 2,2'-bipyridinium isomers (e.g., MV²⁺ and MQ²⁺ in Scheme 3) to generate the substrate radical cation in a Coulombically repulsive environment. (eq 2). However, despite the fact that viologens have been actively explored as herbicides,³ as components of electrochromic display devices,⁴ as acceptors in molecular assemblies designed to store solar energy, as components in supramolecular structures,⁴ and as probes to study DNA⁵ and zeolites⁶ their use as photochemical sensitizers has rarely been explored. This is due in large part to both the absence of photophysical studies⁷ and the lack of readily

SCHEME 1. Monocationic and Dicationic Sensitizers



available viologens and 2,2'-bipyridinium ions with convenient optical and photophysical properties. In addition, only a handful of reports^{8–12} deal with bipyridinium ions with nuclear substituents (on carbon) other than simple alkyl groups or alkyl chains acting as tethers to supramolecular structures, and as a consequence a series of viologens with a range of oxidizing abilities is not available.

Results and Discussion

We report here the synthesis of three new first-generation electronically perturbed 2,2'-bipyridinium ions, **1**, **2**, and **3** (Scheme 2), and preliminary studies on their photophysical and oxidizing properties designed to evaluate their viabilities as electron-transfer sensitizers. We also compare these 2,2'-bipyridinium ions to the more firmly established electron-transfer sensitizer TPP[⊕] that has several attractive features that

(1) *Photoinduced Electron Transfer*; Fox, M. A., Chanon, M., Eds.; Elsevier Science Publishers B. V.: Amsterdam, The Netherlands, 1988.

(2) Miranda, M. A. *Chem. Rev.* **1994**, *94*, 1063–1069.

(3) Summers, L. A. *The Bipyridinium Herbicides*; Academic Press: New York, 1980.

(4) Monk, P. M. S. *The Viologens. Physicochemical Properties, Synthesis and Applications of the Salts of 4,4'-Bipyridine*; John Wiley & Sons: Chichester, England, 1998.

(5) Brun, A. M.; Harriman, A. *J. Am. Chem. Soc.* **1991**, *113*, 8153–8159.

(6) Clennan, E. L. *Coord. Chem. Rev.* **2004**, *248*, 477–492.

(7) For a rare example, see: Peon, J.; Tan, X.; Hoerner, J. D.; Xia, C.; Luk, Y. F.; Kohler, B. *J. Phys. Chem. A* **2001**, *105*, 5768–5777.

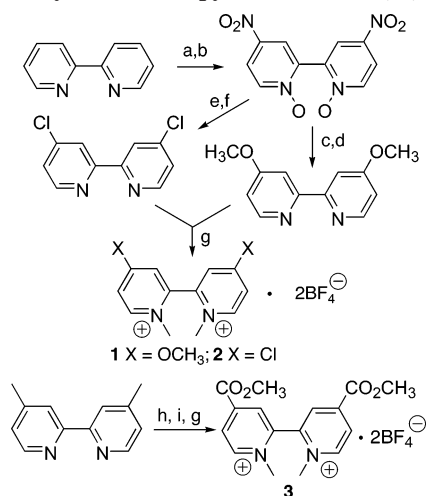
(8) Aziz, D.; Breckenridge, J. G. *Can. J. Res.* **1950**, *28B*, 26–33.

(9) Downes, J. E. *J. Chem. Soc. (C)* **1967**, 2192–2193.

(10) Downes, J. E. *J. Chem. Soc. (C)* **1967**, 1491–1493.

(11) Fielden, R.; Summers, L. A. *Experientia* **1974**, *30*, 843–844.

(12) Pirzada, N. H.; Pojer, P. M.; Summers, L. A. *Z. Naturforsch.* **1976**, *31B*, 115–121.

SCHEME 2. Syntheses of Bipyridinium Ions 1, 2, and 3^a

^a H₂O₂, CH₃COOH, 75 °C. ^bFuming H₂SO₄-HNO₃, 100 °C, 8 h. ^cNaOCH₃, CH₃OH, 30–35 °C, 5 h. ^dPCl₃, CHCl₃, reflux, 5 h. ^eCH₃COCl, CH₃COOH, 100 °C, 4 h. ^fPCl₃, CHCl₃, reflux, 6 h. ^g(CH₃)₃O⁺BF₄⁻, CH₂Cl₂, RT, 36 h. ^hCrO₃, H₂SO₄, 75 °C, 4 h, then RT for 12 h. ⁱH₂SO₄, CH₃OH.

have enhanced its popularity as an electron-transfer sensitizer. These include the following: (1) two absorptions in CH₂Cl₂ at 417 ($\epsilon = 29\,000\text{ L mol}^{-1}\text{ cm}^{-1}$) and 369 nm ($42\,500\text{ L mol}^{-1}\text{ cm}^{-1}$); (2) singlet and triplet energies of 65 and 53 kcal/mol, respectively; (3) its inability to produce ¹O₂ (¹ Δ_g) or superoxide; (4) a large intersystem crossing (*S*₁ → *T*₁) quantum yield of 0.48; and (5) reversible CV reductions in CH₃CN at -0.29 and -1.42 V vs SCE.¹³

The critical step in the syntheses of bipyridinium ions **1**, **2**, and **3** (Scheme 2) is the final alkylation with trimethyloxonium tetrafluoroborate (Meerwein's salt).¹⁴ Early alkylation attempts with methyl iodide met with failure. In the case of the bipyridine precursor to **1** several products presumably from adventitious dealkylation of the methoxy groups were observed.¹⁵ The diminished nucleophilicity of the bipyridine precursors of **2** and **3** precluded reaction, at atmospheric pressure, with methyl iodide even at extended reaction times. The reaction of the bipyridine precursors with Meerwin's salt, however, proceeded to give the bipyridinium ions in excellent yields (**1**, 88%; **2**, 79%; **3**, 84%) after recrystallization from CH₃CN/Et₂O or CH₃CN/ethyl acetate mixtures.

An X-ray crystal structure of **1** is compared to B3LYP DFT calculations in Table 1. Three methoxy rotameric minima were located on the DFT potential energy surface. The X-ray structure corresponds to the *in-out* methoxy conformation which is 2.0 kcal/mol above the DFT *out-out* global minimum (Table 1). The DFT calculations predict, and the X-ray structure confirms, a nearly perpendicular alignment of the two pyridinium rings. The two BF₄⁻ counterions exhibit weak interactions with the bipyridinium nucleus. Both interactions involve a bridging fluorine atom: in one case with a methoxy group (O2–F2 2.778 Å) and in the other case with two nitrogen atoms of adjacent viologen rings (N2–F5 3.211 Å and N1A–F5 3.128 Å) as denoted by the dotted lines in the structure in Table 1.

(13) Saeva, F. D.; Olin, G. R. *J. Am. Chem. Soc.* **1980**, *102*, 299–303.

(14) Meerwein, H. In *Organic Syntheses*; Baumgarten, H. E., Ed.; John Wiley & Sons: New York, 1973; Collect. Vol. V, pp 1096–1098.

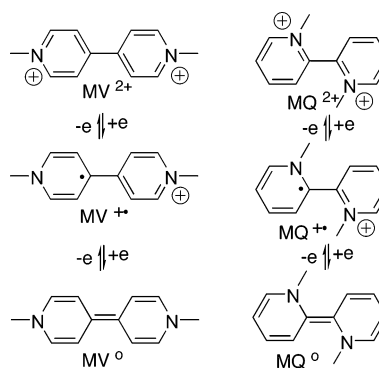
(15) Pojer, P. M.; Summers, L. A. *J. Heterocycl. Chem.* **1974**, *11*, 303–305.

TABLE 1. Comparison of DFT and X-ray Structures of 1^a

	<i>E</i> _{rel} , kcal/mol	<i>d</i> (C ₆ –C ₇), Å	θ (C ₅ C ₆ C ₇ C ₈), deg
X-ray		1.494(3)	81.9(3)
1 (out-out) ^b	0	1.501	88.06
1 (in-out)	2.0	1.502	85.44
1 (in-in)	4.1	1.503	86.62

^a DFT calculations at the B3LYP/6-31G(d) level. ^b Out and in refer to the C₁₃O₁C₄C₅ or C₁₄O₂C₉C₈ dihedral angle of near 180° and 0°, respectively.

SCHEME 3. Viologen and 2,2'-Bipyridinium Ion Redox States



Perhaps the single most important feature of viologens and 2,2'-bipyridinium ions is their ability to exist in three well-defined oxidation levels. These redox states have been most exhaustively explored with the 4,4'-bipyridinium ion, methyl viologen MV²⁺, which exhibits two reversible reductions at -0.45 and -0.86 V versus SCE.⁴ Structures for similar oxidation states for the 2,2'-bipyridinium ions **1**, **2**, and **3** can also be drawn (Scheme 3). However, preliminary electrochemical studies (Figure 1) illustrate that only **3** shows two reversible one-electron reductions reminiscent of the 4,4'-bipyridinium ions. All the CV's were collected under an argon atmosphere although only **1**^{•+} is thermodynamically competent to reduce oxygen ($E_{1/2}^{\text{Red}}(\text{oxygen}) = -0.86\text{ V vs SCE in CH}_3\text{CN}$).¹⁶ We attribute the apparent instability of MQ^{•+} (Scheme 3) to steric effects that prevent formation of the electronically preferred planar radical cation. B3LYP/6-31G(d) DFT studies also show that **3**^{•+} is nonplanar; however, the carbomethoxy groups must provide sufficient resonance interaction to produce a radical cation stable on the cyclic voltammetry time scale. Bipyridinium

(16) Sawyer, D. T. *Oxygen Chemistry*; Oxford University Press: New York, 1991.

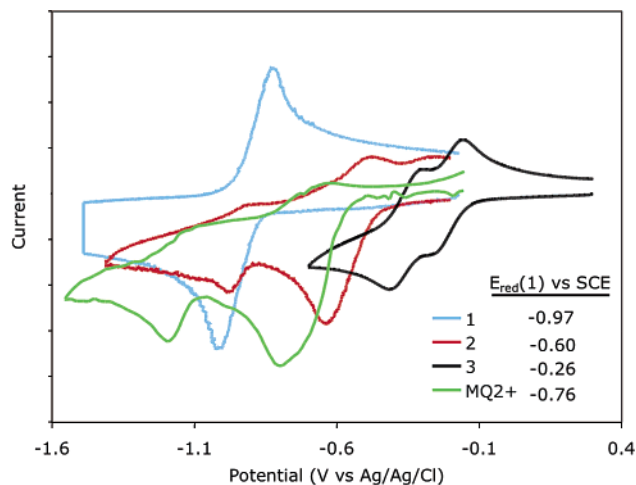


FIGURE 1. Cyclic voltammograms for **1**, **2**, **3**, and MQ²⁺.

TABLE 2. Optical Data for 2,2'-Bipyridinium Ions **1**, **2**, and **3**

	λ^{ABS} (ϵ) ^a	λ^{F} ^b	Φ_{F} ^c	λ^{P} ^e
1	212 (40 800)	345	0.0010 ± 0.0004	392
	251 (33 200)			
2	200 (41 200)	332	0.012 ± 0.002	425
	241 (24 100)			
	263 (11 900)			
	271 (13 800)			
3	224 (26,200)	<i>d</i>		432
	285 (17 900)			

^a Absorption maxima, λ^{ABS} , in nm; extinction coefficient, ϵ , in $\text{L mol}^{-1} \text{cm}^{-1}$ in CH_3CN . ^b Fluorescence maximum in CH_3CN . ^c Fluorescence quantum yield in CH_3CN versus anthracene in ethanol ($\Phi_{\text{F}} = 0.27 \pm 0.03$). ^d Not observed. ^e Phosphorescence maximum in ethanol glass at 77 K.

ion **1** gives a single 2-electron reduction, as determined coulometrically, at -0.97 V versus SCE, while **2** exhibits two CV peaks with only a hint of reversibility.

Despite this wide spectrum of electrochemical behavior we note that the substituents provide the anticipated electronic effect on the formation of the radical cations since the reduction potentials given in Figure 1 are linearly related to the Hammett substituent constants ($E_{\text{red}}(1) = 0.95\sigma_{\text{p}} - 0.745$; $r^2 = 0.9631$).

Optical data collected for bipyridinium ions **1**, **2**, and **3** are given in Table 2. Unfortunately, all of the bipyridinium ions absorb at considerably shorter wavelengths than TPP[⊕]. Addition of 2,3-dimethyl-2-butene to the 2,2'-bipyridinium ions resulted in formation of a shoulder on the red edge of each absorption spectrum consistent with charge transfer (CT) formation. Benesi–Hildebrand analysis¹⁷ of the charge-transfer complexes in CH_3CN gave equilibrium constants (**1**, $0.16 \pm 0.06 \text{ M}^{-1}$; **2**, $0.58 \pm 0.08 \text{ M}^{-1}$; **3**, $0.20 \pm 0.03 \text{ M}^{-1}$) of the same order of magnitude as observed previously for MQ²⁺.¹⁸ The lack of correlation of K_{eq} with the electronic character of the substituent suggests that steric effects also play a role in the stabilities of these CT complexes.

2,2'-Bipyridinium ions **1** and **2**, but not **3**, also generate very weak fluorescence at approximately 345 and 332 nm, respectively. The excellent agreement between the ground-state absorption and the excitation spectra for both **1** and **2** confirms

the fluorescence origin of this emission. This confirmation is important in view of the controversial emission from MV²⁺ that has been attributed, by some authors, to adventitious pyridone oxidation products.¹⁹ Only recently has a femtosecond laser flash photolysis study provided convincing evidence for fluorescence from ¹MV^{2+*} in acetonitrile.⁷

The quantum yields of fluorescence, Φ_{F} (Table 2), were determined by comparison with anthracene in ethanol ($\Phi_{\text{F}} = 0.27 \pm 0.03$) and are considerably smaller than the values of 0.04 ± 0.02 reported for 1,1'-ethylene-2,2'-bipyridinium dibromide in water²⁰ or of 0.03 ± 0.01 reported for MV²⁺ in acetonitrile.^{8–12} We estimate that the S₁ energies for both **1** and **2** are approximately 99 kcal/mol from intersection of the corrected emission and absorption spectra at 290 nm. The singlet energies are considerably larger than that observed for TPP[⊕] (vide supra) and slightly larger than that reported for MV²⁺ (95 kcal/mol).^{8–12} A direct consequence of these high excited singlet state energies is that these viologens function as more potent photochemical oxidants than ¹TPP^{⊕*}. For example, since ΔG° (kcal mol⁻¹) for electron transfer is given by $23.06(E_{\text{Ox}}(\text{donor}) - E_{\text{Red}}(\text{acceptor}) - \Delta E_{\text{Singlet}})$, ¹TPP^{⊕*} is thermodynamically capable of oxidizing substrates (donors) with oxidation potentials less than 2.5 V vs SCE while ¹I⁺ can oxidize substrates with E_{Ox} as high as 3.32 V vs SCE.

Figure 2 shows transient absorption spectra collected 0.56 and 0.28 μs after irradiation of 0.1 mM solutions of **2** and **3**, respectively, with 266 nm pump pulses from a Nd:YAG laser. The absorption spectra exhibit valleys that we attribute to bleaching of **2** and **3** and absorption bands at approximately 430 and 450 nm, respectively. In samples rigorously degassed by a series of freeze–thaw cycles at 10^{-4} Torr these signals decay by first-order processes (insets in Figure 2) with lifetimes of 22 ± 1 (**2**) and $4.8 \pm 0.5 \mu\text{s}$ (**3**). The signals do not decay completely to the baseline and small residual signals (see insets in Figure 2) exist out to the millisecond time regime.

Photoreduction of MV²⁺ has been reported in zeolites, in methanol,^{20,21} and as the chloride salt under conditions which favor tight ion pairing. However, we can rule out the reduction products, **2**⁺ and **3**⁺, as the species responsible for the transient absorption spectra (Scheme 5) for several reasons: (1) The observed lifetimes are inconsistent with the cyclic voltammetry results which require substantially longer lifetimes for the radical cations, (2) RPA/6-31G(d) calculations predict that MQ⁺ should absorb at 985 nm.¹⁸ It is unlikely that substituent effects could be responsible for over a 500 nm hypsochromic shift, and (3) despite the fact that **2**⁺ and **3**⁺ are thermodynamically precluded from producing superoxide, oxygen dramatically enhances the rate of decay of the transients. Consequently, as an alternative we assign the observed transients as triplet–triplet absorption spectra. This assignment is confirmed by the observation that **1** is capable of sensitizing the singlet oxygen ene reaction of 2,3-dimethyl-2-butene to give the allylic hydroperoxide product.^{22,23} It is also consistent with the oxygen quenching results and the observation of phosphorescence at 77 K (Table 1).

(19) Mau, A. W.-H.; Overbeek, J. M.; Loder, J. W.; Sasse, W. H. F. *J. Chem. Soc. Faraday Trans. 2* **1986**, 82, 869–876.

(20) Hopkins, A. S.; Ledwith, A.; Stam, M. F. *J. Chem. Soc., Chem. Commun.* **1970**, 494–495.

(21) Ledwith, A. *Acc. Chem. Res.* **1972**, 5, 133–139.

(22) Clennan, E. L. *Tetrahedron* **2000**, 56, 9151–9179.

(23) Clennan, E. L. In *Synthetic Organic Photochemistry*; Marcel Dekker: New York, 2005; pp 365–390.

(17) Benesi, H. A.; Hildebrand, J. H. *J. Am. Chem. Soc.* **1949**, 71, 2703–2707.

(18) Pace, A.; Clennan, E. L.; Jensen, F.; Singleton, J. *J. Phys. Chem. B* **2004**, 108, 4673–4678.

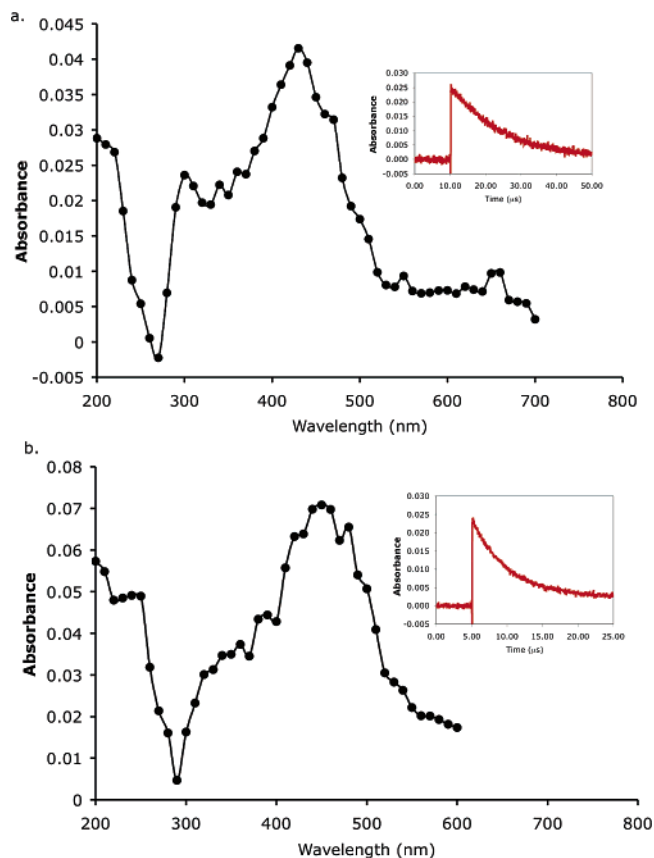


FIGURE 2. Nanosecond laser flash photolysis data for **2** and **3**. Transient absorption spectra and decay profiles (inset) for (a) **2** and (b) **3** in CH_3CN monitored at 450 nm for **2** and 460 nm for **3**.

We estimate from the phosphorescence spectra that the triplet energies are approximately 75–80 kcal/mol. Consequently, the triplets should be capable of oxidizing substrates with oxidation potentials less than 3.0 V vs SCE.

Conclusion

We have reported the synthesis of three new first-generation 2,2'-bipyridinium salts with electronically perturbing substituents directly attached to the carbons in the pyridinium core. An optical study of these new compounds has resulted in the first example of triplet–triplet absorption spectra of 2,2'-bipyridinium ions and electrochemical properties that span a convenient potential range. However, their absorption maxima are substantially hypsochromic of the more widely used pyrylium salts decreasing their utility as electron transfer sensitizers. Consequently, syntheses and characterizations of new second-generation electron transfer sensitizers bathochromatically shifted from typical substrate absorbances are currently underway and will be reported soon.

Experimental Section

4,4'-Dimethoxy-1,1'-dimethyl-2,2'-bipyridinium Tetrafluoroborate (1).²⁴ A mixture of 4,4'-dimethoxy-2,2'-bipyridine (0.001 mol) and trimethyloxonium tetrafluoroborate (0.002 mol) in 30 mL of dichloromethane was stirred at room temperature for 36 h. The

solvent was evaporated in vacuo and the product recrystallized three times from CH_3CN and ethyl acetate to give colorless crystal. Yield: 0.37 g (0.88 mmol, 88%). Mp: 195–196 °C. ^1H NMR (400 MHz; D_2O , ppm): δ 8.86 (d, $J = 7.3$ Hz, 2H), 7.76 (d, $J = 3.0$ Hz, 2H), 7.72 (dd, $J = 7.3$ and 3.0 Hz, 2H), 4.18 (s, 6H), 3.97 (s, 6H). ^1H NMR (400 MHz; CD_3CN , ppm): δ 8.69 (d, $J = 6.8$ Hz, 2H), 7.63 (m, 4H), 4.17 (s, 6H), 3.89 (s, 6H). ^{13}C NMR (100 MHz; CD_3CN , ppm): δ 173.1 (s), 151.0 (d, $J_{\text{C-H}} = 193$ Hz), 145.8 (s), 118.3 (d, $J_{\text{C-H}} = 175$ Hz), 115.9 (d, $J_{\text{C-H}} = 176$ Hz), 59.9 (q, $J_{\text{C-H}} = 149$), 46.4 (q, $J_{\text{C-H}} = 146$ Hz). IR: ν_{max} (KBr pellet) 3090 (w), 1640 (m), 1520 (m), 1280 (m), 1060 (s) cm^{-1} . Anal. Calcd for $\text{C}_{14}\text{H}_{18}\text{N}_2\text{O}_2\text{B}_2\text{F}_8$: C, 40.04; H, 4.32; N, 6.67. Found: C, 40.30; H, 4.27; N, 6.61.

4,4'-Dichloro-1,1'-Dimethyl-2,2'-bipyridinium Tetrafluoroborate (2).²⁴ A mixture of 4,4'-dichloro-2,2'-bipyridine (0.001 mol) and trimethyloxonium tetrafluoroborate (0.002 mol) in 30 mL of dichloromethane was stirred at room temperature for 48 h. The solvent was evaporated in vacuo and the product recrystallized three times from CH_3CN and diethyl ether to give a white product. Yield: 0.34 g (0.79 mmol, 79%). Mp > 225 °C. ^1H NMR (400 MHz; CD_3CN , ppm): δ 8.94 (d, $J = 6.8$ Hz, 2H), 8.38 (dd, $J = 6.7$ and 2.5 Hz, 2H), 8.25 (d, $J = 2.3$ Hz, 2H), 4.07 (s, 6H). ^1H NMR (400 MHz; D_2O , ppm): δ 9.19 (d, $J = 6.1$ Hz, 2H), 8.49 (m, 4H), 4.19 (s, 6H). ^{13}C NMR (100 MHz; CD_3CN , ppm): δ 156.9 (s), 151.4 (d, $J_{\text{C-H}} = 198$ Hz), 144.0 (s), 133.2 (d, $J_{\text{C-H}} = 188$ Hz), 132.5 (d, $J_{\text{C-H}} = 182$ Hz), 48.8 (q, $J_{\text{C-H}} = 148$ Hz). IR: ν_{max} (KBr pellet) 3100 (m), 1620 (m), 1060 (s) cm^{-1} . Anal. Calcd for $\text{C}_{12}\text{H}_{12}\text{N}_2\text{B}_2\text{F}_8\text{Cl}_2$: C, 33.62; H, 2.82; N, 6.53. Found: C, 33.73; H, 2.77; N, 6.52.

1,1'-Dimethyl-4,4'-dicarbomethoxy-2,2'-bipyridinium Tetrafluoroborate (3).²⁴ A mixture of 4,4'-dicarbomethoxy-2,2'-bipyridine (0.001 mol) and trimethyloxonium tetrafluoroborate (0.002 mol) in 30 mL of dichloromethane was stirred at room temperature for 36 h. The solvent was evaporated in vacuo and the product recrystallized three times from CH_3CN and ethyl acetate to give white crystal. Yield: 0.40 g (0.85 mmol, 84%). Mp: 150 °C dec. ^1H NMR (400 MHz; CD_3CN , ppm): δ 9.20 (d, $J = 6.3$ Hz, 2H), 8.73 (dd, $J = 6.3$ and 2.0 Hz, 2H), 8.66 (d, $J = 1.9$ Hz, 2H), 4.15 (s, 6H), 4.05 (s, 6H). ^{13}C NMR (100 MHz; CD_3CN , ppm): δ 162.9 (s), 152.5 (d, $J_{\text{C-H}} = 201$ Hz), 147.6 (s), 144.7 (s), 131.8 (d, $J_{\text{C-H}} = 174$ Hz), 131.4 (d, $J_{\text{C-H}} = 179$ Hz), 55.3 (q, $J_{\text{C-H}} = 149$ Hz), 49.6 (q, $J_{\text{C-H}} = 148$ Hz). IR: ν_{max} (KBr pellet) 1750 (s), 1300 (m), 1070 (s), 768 (m), 525 (s) cm^{-1} . Anal. Calcd for $\text{C}_{16}\text{H}_{18}\text{N}_2\text{O}_4\text{B}_2\text{F}_8$: C, 40.38; H, 3.81; N, 5.89. Found: C, 40.08; H, 3.76; N, 5.74.

Fluorescence Quantum Yield Determinations. The quantum yields were determined by the method of Eaton.²⁵ The quantum yield of the fluorescence standard, anthracene, in ethanol ($\Phi_{\text{A}} = 0.27 \pm 0.03$)^{10,25} was used in conjunction with the equation $\Phi_{\text{F}} = [(A_{\text{A}}F_{\text{V}}n^2)/(A_{\text{V}}F_{\text{A}}n_0^2)]\Phi_{\text{A}}$ to determine the quantum yield of 2,2'-bipyridinium ion fluorescence, Φ_{F} , where A_{A} and A_{V} are the absorbance at the excitation wavelength, F_{A} and F_{V} are the integrated emission area across the band, of anthracene and the viologen, respectively, and n_0 and n are the index of refraction of ethanol (1.3600) and acetonitrile (1.3410), respectively. The absorbances of the 2,2'-bipyridinium ions and anthracene were adjusted to be similar and below 0.10. The reported results are the average of three independent determinations. Anthracene in ethanol: slit width = 2.5 nm, excitation wavelength = 345 nm, $A_{345\text{nm}} = 0.09546$, $F = 8020$. 2,2'-Bipyridinium ion, **1**, in acetonitrile: slit width = 2.5 nm, excitation wavelength = 253 nm, $[\mathbf{1}] = 3.12 \times 10^{-6}$ M, $A_{253\text{nm}} = 0.1000$, $F = 32$. 2,2'-Bipyridinium ion, **2**, in acetonitrile: slit width = 2.5 nm, excitation wavelength = 272 nm, $[\mathbf{2}] = 3.90 \times 10^{-6}$ M, $A_{272\text{nm}} = 0.0553$, $F = 209$.

X-ray Structure of 1. X-ray diffraction data from a crystal of **1** obtained by slow crystallization from 1:1 CH_3CN :ethyl acetate

(24) Negele, S.; Wieser, K.; Severin, T. *J. Org. Chem.* **1998**, *63*, 1138–1143.

(25) Eaton, D. F. In *CRC Handbook of Organic Photochemistry*; Scaiano, J. C., Ed.; CRC Press: Boca Raton, FL, 2000; Vol. I, pp 231–239.

were collected on a diffractometer employing Mo K α radiation (graphite monochromator) at -100 °C. Standard control and integration and structure solution, refinement, and graphics software were employed. The unit cell parameters were obtained from a least-squares fit to the angular coordinates of all reflections. Intensities were integrated from a series of frames (0.3° ω rotation) covering more than a hemisphere of reciprocal space. Absorption and other corrections were applied.

1 crystallizes in the orthorhombic space group, *Pbca*. The asymmetric unit consists of the bipyridinium cations and two BF $_4^-$ anions. All of them are well-ordered and situated on general positions. All non-hydrogen atoms were located in the Fourier maps and refined anisotropically. All H atoms were placed in calculated positions and refined isotropically by a riding model.

Phosphorescence Spectra. Low-temperature phosphorescence spectra were obtained with a resolution of ± 1 nm at 77 K, using the pulsed source and gated detection in a spectrometer equipped with a low-temperature accessory. The delay times were set at 0.1 ms and gate times at 9.9 ms for each sample. The emission data

(26) *Handbook of Analytical Chemistry*; McGraw Hill: New York, 1963; Section 5.

(27) Frisch, M. J.; Trucks, G. W.; Schlegel, H. B.; Scuseria, G. E.; Robb, M. A.; Cheeseman, J. R.; Montgomery, J. A., Jr.; Vreven, T.; Kudin, K. N.; Burant, J. C.; Millam, J. M.; Iyengar, S. S.; Tomasi, J.; Barone, V.; Mennucci, B.; Cossi, M.; Scalmani, G.; Rega, N.; Petersson, G. A.; Honda, H.; Kitao, O.; Nakai, H.; Klene, M.; Li, X.; Knox, J. E.; Hratchian, H. P.; Cross, J. B.; Adamo, C.; Jaramillo, J.; Gomperts, R.; Stratmann, R. E.; Yazyev, O.; Austin, A. J.; Cammi, R.; Pomelli, C.; Ochterski, J. W.; Ayala, P. Y.; Morokuma, K.; Voth, G. A.; Salvador, P.; Dannenberg, J. J.; Zakrzewski, V. G.; Dapprich, S.; Daniels, A. D.; Strain, M. C.; Farkas, O.; Malick, D. K.; Rabuck, A. D.; Raghavachari, K.; Foresman, J. B.; Ortiz, J. V.; Cui, Z.; Baboul, A. G.; Clifford, S.; Cioslowski, J.; Stefanov, B. B.; Liu, G.; Liashenko, A.; Piskorz, P.; Komaromi, I.; Martin, R. L.; Fox, D. J.; Keith, T.; Al-Laham, M. A.; Peng, C. Y.; Nanayakkara, A.; Challacombe, M.; Gill, P. M. W.; Johnson, B.; Chen, W.; Wong, M. W.; Gonzalez, C.; Pople, *Gaussian 03*, Revision A.1; Gaussian, Inc., Pittsburgh, PA, 2003.

were collected with use of slit widths of 5 nm and with PMT voltages set at 775 V. Samples were prepared and the data collected in absolute ethanol that had been purified by atmospheric distillation through a 1 m column packed with glass beads. The sample concentrations were 2×10^{-6} , 2×10^{-6} , and 8×10^{-6} M for **1**, **2**, and **3**, respectively. Phosphorescence data were collected by excitation at 2540, 2720, and 2900 Å for samples **1**, **2**, and **3**, respectively. The phosphorescence spectra were generated from these data by subtracting background emission data from ethanol blanks excited at identical wavelengths.

Cyclic Voltammetry. Data were collected at 1000 mV/s (250 mV/s for **3**) in acetonitrile with samples 2×10^{-3} M in substrate and 0.1 M in tetra-*n*-butylammonium perchlorate on a Potentiostat/Galvanostat. The working electrode was glassy carbon and the counter electrode was a platinum wire. The reference electrode was Ag/AgCl 0.1 M KCl in water, which were converted to SCE by subtraction of 0.047 V.²⁶ Preliminary work at different scan rates has also been done. Expected changes as anticipated for irreversible and quasireversible systems were observed.

DFT Calculations. DFT calculations were done with Gaussian 03²⁷ and the characters of all stationary points were verified by frequency calculations.

Acknowledgment. We thank the National Science Foundation (CHE-0313657) for the generous support of this research. We also thank Sean Hightower for assistance in the DFT calculations.

Supporting Information Available: Synthetic procedures, several ORTEP views of crystal and unit cell, and Z-matrix and total energies for calculations, as well as a CIF file for the crystal structure of **1**. This material is available free of charge via the Internet at <http://pubs.acs.org>.

JO052127I